NANOSYSTEMS:
PHYSICS, CHEMISTRY, MATHEMATICS

Glebova N.V., et al. *Nanosystems: Phys. Chem. Math.*, 2023, **14** (2), 202–207.
http://nanojournal.ifmo.ru
DOI 10.17586/2220-8054-2023-14-2-202-207

Original article

Investigation of stability of composite Nafion/nanocarbon material

Nadezhda V. Glebova[1,a], Anton S. Mazur[2,b], Anna O. Krasnova[1,c], Ivan V. Pleshakov[1,d], Andrey A. Nechitailov[1,e]

[1]Ioffe Institute, St. Petersburg, Russia

[2]St. Petersburg State University, St. Petersburg, Russia

[a]glebova@mail.ioffe.ru, [b]a.mazur@spbu.ru, [c]krasnova@mail.ioffe.ru, [d]inanple@yandex.ru, [e]aan.shuv@mail.ioffe.ru

Corresponding author: Nadezhda V. Glebova, glebova@mail.ioffe.ru

PACS 61.46.+w; 82.33.Pt; 68.35.Dv

ABSTRACT The article presents the results of a study of inorganic-polymer nanocomposites Nafion/thermally expanded graphite and Nafion/carbon black by nuclear magnetic resonance and thermogravimetry. The structure of carbon materials was characterized by electron microscopy and adsorption structural analysis by low-temperature nitrogen adsorption. The presence of the interaction of Nafion polymer and carbon material at the interface between the components leading to thermal stabilization of the composites is shown, and the differences between thermally expanded graphite and carbon black due to their morphology during interaction with Nafion are discussed.

KEYWORDS composite stability, Nafion migration, graphene, carbon black, NMR, thermogravimetry.

ACKNOWLEDGEMENTS The work was supported by the grant from the Russian Science Foundation No. 22-23-20127, https://rscf.ru/project/en/22-23-20127/ and the grant from the St. Petersburg Science Foundation in accordance with the agreement of 14.04.2022 No. 28/2022.

FOR CITATION Glebova N.V., Mazur A.S., Krasnova A.O., Pleshakov I.V., Nechitailov A.A. Investigation of stability of composite Nafion/nanocarbon material. *Nanosystems: Phys. Chem. Math.*, 2023, **14** (2), 202–207.

1. Introduction

Inorganic-polymer composites have recently been increasingly used in various fields of technology. One such application is the use of nanocomposites containing the Nafion proton-conducting polymer and a carbon material (usually carbon black) with catalyst nanoparticles on the surface for electrochemical energy conversion devices such as fuel cells, electrolyzers, etc. This is a fairly wide range of products, including various low-temperature fuel cells and water electrolyzers [1]. The reduction in cost and increase in the competitiveness of such devices is largely due to the solution of the problem of their durability. The related new knowledge about degradation mechanisms should serve both as a theoretical and practical basis for further development of membrane electrode assemblies (MEA).

A significant number of works have been devoted to the study of degradation processes in the MEA. Note that, despite the fact that the historical depth of publications is estimated at an impressive period of more than 10 years, the service life of modern MEAs is still not long enough and is about 5000 hours with a voltage loss of about 10% of the original one. Aging is associated with common electrochemical processes, such as electrochemical and chemical oxidation of the carbon and metal components of the electrode, recrystallization of metals, ingrowth of metal dendrites into the proton-conducting membrane, violation of the integrity of the membrane due to chemical and electrochemical oxidation-reduction processes [2–9].

One of the reasons for the deterioration of the characteristics of a fuel cell with a proton-conducting membrane is the migration of Nafion in the electrode, as a result of which inhomogeneity appears and the resistance to proton transfer increases [10]. The creation of new methods for extending the service life of electrochemical devices based on MEA containing Nafion is an urgent task.

Another promising field of application of inorganic-polymer composites is the elaboration of anti-radar coatings. In addition to the requirements associated with their functional properties, some of them are related to the microstructure and also physical and operational characteristics. For example, review [11] notes that an ideal shielding material should demonstrate high attenuation over a wide frequency range, low density, good thermal stability, and low cost. An important feature is the presence of good characteristics in high temperature conditions, which result from aerodynamic heating. Various carbon-based structures, having these properties and, in particular, the ability to strongly absorb electromagnetic waves, have attracted much attention as possible coatings of this kind. The use of substances such as carbon black [12], carbon nanotubes [13], carbon fibers [14], biomass carbon [15], graphite [16], and graphene-like materials [17, 18] has been considered. A possible way to create anti-radar coatings is utilizing of conducting polymers as matrices for the

embedded carbon nanoobjects [19, 20]. For example, in [19], a single-layer absorber based on a phenol resin reinforced with a polyaniline/expanded graphite composite, synthesized by *in situ* polymerization of aniline in an acidic medium, was studied. It was shown that attenuation in such a medium increases in the microwave range.

A negative factor in the synthesis of inorganic-polymer composites degrading their absorbing characteristics is the agglomeration of nanoparticles of the embedded material, which not only violates microhomogeneity, but also reduces the surface area of the dispersed component.

Composites based on the proton-conducting polymer Nafion and nanostructured carbon materials are relatively poorly studied [20], but they seem perspective both in terms of providing a stable homogeneous microstructure (since Nafion has pronounced surface-active properties and stabilizes nanosized carbon structural elements, preventing their agglomeration) and also because of their anti-corrosion performance [21]. In addition, the intercalation of carbon materials into the composite enhances the thermal stability of Nafion [22].

Thus, inorganic-polymer composites have great potential for practical application in various fields, although there is a problem of their stability. Due to the combination of ionic conductivity, surface active properties, and the ability to inhibit corrosion, Nafion is of particular interest for use in composites with carbon materials. Carbon nanomaterials have different formation at the micro level, which determines many of their structure-dependent properties. So, graphene is often considered as a pseudo-two-dimensional material, while carbon black is a conventional three-dimensional material. Due to this, different influence of these materials on the characteristics of the composite is expected.

The goal of this work is to study the causes and features of the stabilizing effect in a composite containing a dispersed phase of carbon nanostructured materials of various morphologies: pseudo-two-dimensional low-layer graphene and three-dimensional carbon black in the Nafion polymer medium.

2. Materials and experimental technique

In the work, thermally expanded graphite (TEG) obtained by the technology described in [23] (NP Tomsk Atomic Center) and commercial carbon black of the Vulcan XC-72 type were used as a carbon filler. The polymer matrix was obtained from a solution of Nafion brand DE1021 (DuPont). For the thermogravimetric study of Nafion, an aqueous isopropanol solution was prepared - isopropanol (99.80%, special purity, EKOS-1 JSC) with a content of 2 wt. % Nafion; the solution was dried on glass under normal conditions to an air-dry state (relative humidity ∼40–50%), and then the dry residue was removed with a spatula.

Nafion/TEG and Nafion/Vulcan two-component composites were made by mixing precise weights of the components in isopropanol/watermixture, taken in 1:1 volume ratio, followed by mechanical stirring and ultrasonic homogenization. The ratio of solid and liquid phases in the dispersion was maintained within (1:40)–(1:80) depending on the content of the carbon component. The higher the content of the latter, the more the liquid phase was added to ensure complete wetting of the solid components. The treatment was carried out in a Branson 3510 bath at an ultrasound operating frequency of 40 kHz and a power of 130 W for about 30–50 h until a visually homogeneous dispersion was obtained. The dispersion was dried on glass under normal conditions to an air-dry state (∼40–50% relative humidity) with subsequent removal of dry residue.

The carbon materials used in the work were characterized by electron microscopy and adsorption-structural analysis by low-temperature nitrogen adsorption.

Microscopic studies were carried out using electron microscopes Quanta 200 and JEM-2100F and at the Engineering Center of St. Petersburg State Institute of Technology on TESCAN and VEGA 3 SBH.

The morphology of carbon materials was studied using the ASAP 2020 specific surface analyzer. The specific surface area of the sample (S_{sp}), specific volume (V_{sp}) of pores, size, and pore size distribution were calculated using the BET method. Bulk density and specific pore volume were determined independently by gravimetric technique.

NMR experiments were performed on the equipment of the resource Center for Magnetic Resonance of St. Petersburg State University as follows. On a Bruker AVANCE III WB 400 spectrometer (magnetic field strength 9.4 T), the responses of ^{1}H, ^{19}F, and ^{13}C nuclei were recorded, the operating frequencies for which are 400, 376, and 104 MHz, respectively. The sample was placed in a probe - zirconium oxide rotor with an outer diameter of 4 mm, rotating at a magic angle with different frequencies (usually 12.5 kHz, although in some cases it was not possible to achieve this value due to the high conductivity of the substance). For the spectra of fluorine, several frequencies were used to determine the isotopic components of the spectrum. Tetramethylsilane was taken as an external reference for the ^{1}H and ^{13}C nuclei, and a one-molar aqueous solution of lithium fluoride was used for the ^{19}F nuclei. To excite the resonance, a single-pulse sequence with a pulse duration and a relaxation delay of 2.5 μs and 30 s for ^{1}H, 1.2 μs and 30 s for ^{13}C, and 2.9 μs and 2 s for ^{19}F, respectively, was used.

The thermal stability of the composites was studied on a Mettler-ToledoTGA/DSC 1 derivatograph with STAReSystem software. A sample of the material (2–3 mg) was placed in alundum crucible located in the instrument chamber. Registration of thermogravimetric curves (TG) was performed with air blowing through the chamber at a flow rate of 30 cm^3 min^{-1} in the mode of monotonic temperature rise at a rate of 5 K min^{-1} in the range of 35–1000°C.

TABLE 1. Structural characteristics of the investigated carbon materials

Material	Bulk density, g/cm^3	Porosity, %	Specific pore volume over the entire size range (including macropores), cm^3·g^{-1}	Specific surface area, m^3/g
TEG	0.002	99.9	500	143
Vulcan XC-72	0.26	88.0	1.7	200 – 250

3. Results and discussion

Micrographs of the studied carbon materials are shown in Fig. 1, from which it can be seen that they have a significantly different structure. Fig. 1a demonstrates the flakes of the initial TEG. It should be noted that this material has a very small bulk density (see Table 1), and after dispersion in isopropanol-water-Nafion medium, a homogeneous dispersion consisting of smaller graphene structures forms, up to graphene containing 1–3 layers [24]. The TEG (Fig. 1a, Fig. 1b) is built from graphene planes, while Vulcan (Fig. 1c, Fig. 1d) consists of spherical globules with a size in the range of about 60–100 nm.

Some structural characteristics of the carbon materials are given in Table 1. As follows from it, in the initial state both of them have a fairly close specific surface area, however, the porosity of TEG is significantly higher, which is explained by the peculiarities of its microcomposition: a system of flakes in the form of fused petals.

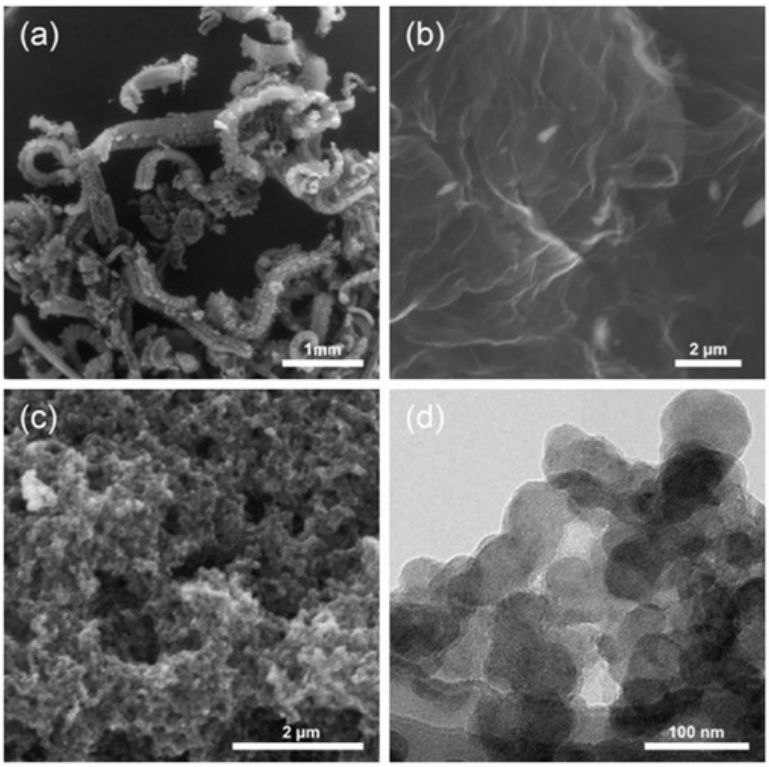

FIG. 1. Micrographs of the carbon materials: (a) SEM image of thermally expanded graphite flakes, (b) SEM image of the structure of thermally expanded graphite, (c) SEM image of Vulcan, (d) TEM image of Vulcan

The ^{1}H NMR spectra of the samples under study are shown in Fig. 2 (for Nafion/TEG, Nafion/Vulcan, and for pure Nafion in Figs. 2a, b and c respectively). Note that the signal-to-noise ratio for composites with carbon materials is much lower than for pure Nafion, which is owing to the presence of a conductive carbon phase and, consequently, a decrease in the Q-factor of the resonant circuit. It can be seen that the pure polymer Nafion has narrow intense inhomogeneously broadened spectral line with a chemical shift of 7.3 ppm (Fig. 2c), typical for water molecules in ionized pores of Nafion. This line is not observed in composites. Nafion/TEG exhibits a broad unresolved line with a maximum of about 1.7 ppm (Fig. 2a), which may be associated with a fast relaxation rate due to the presence of a highly conductive phase in the sample. The Nafion/Vulcan spectrum contains three broadened components with shifts of about 5.7, 1.3, and - 6.5 ppm, as well as a low-intensity peak of about 4.5 ppm (Fig. 2b). The narrow line is characteristic for free water, which could be

released from the sample mass under the influence of the rotation. The line of about 5.7 ppm most likely corresponds to the signal of water in the pores of Nafion with a lower degree of their intrapore ionization. A shift of the proton response to the negative region of the spectrum (as in the resonance near - 6.5 ppm) can be observed in cases when the hydrogen atom is additionally shielded (for example, it is located in a metal or other conductive matrix).

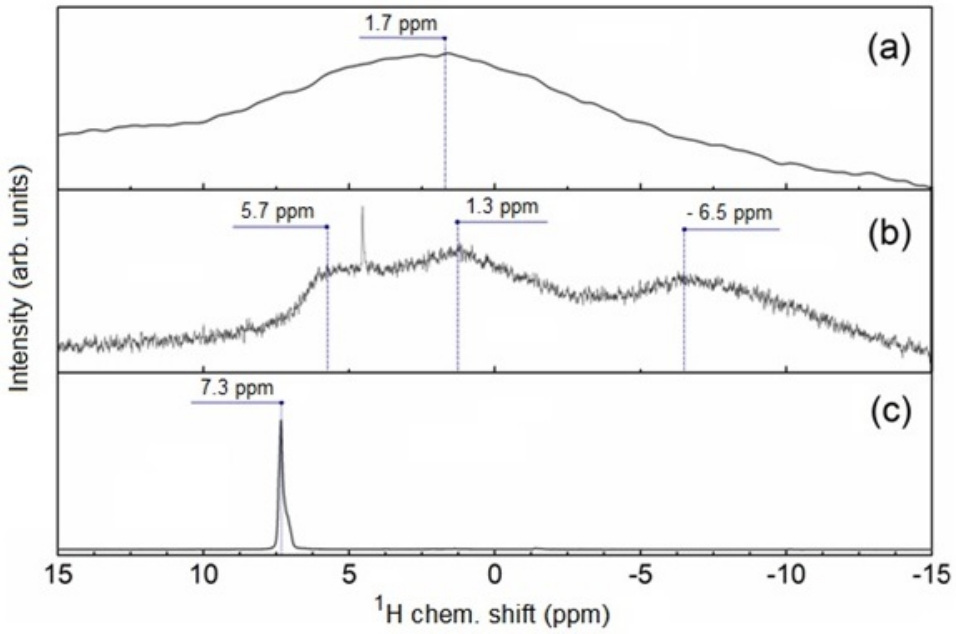

FIG. 2. Solid-state NMR spectra on the nuclei of ^{1}H of composite Nafion/carbon materials (wt. : wt.): a) Nafion/TEG 1 : 4; b) Nafion/Vulcan 1 : 4; c) Nafion 1 : 0

NMR spectra on ^{13}C nuclei have a wide unresolved line of about 111 ppm for pure Nafion and a broadened line in the region of the same chemical shift for the composition of Nafion/Vulcan. For the Nafion/TEG sample, the ^{13}C NMR spectrum could not be registered.

In all samples, the signals of ^{19}F were registered with a set of spectral components characteristic of Nafion. For Nafion and Nafion/Vulcan, the components – 80 ppm (OCF_2 and CF_3), – 117 ppm (SCF_2), – 122 ppm ((CF_2)n), – 138 ppm(CF(b)) and – 144 ppm (CF(s)) were resolved [25]. In Nafion/TEG, one unresolved broadened line was observed with a maximum of about – 122 ppm.

A significant broadening of the NMR lines from the ^{1}H and ^{19}F nuclei, as well as the impossibility of registering the ^{13}C spectrum for the Nafion/TEG sample, is associated with the high conductivity of TEG, which leads to a decrease in the Q-factor of the resonant circuit and/or to acceleration of relaxation processes. On the other hand, the presence of Vulcan particles in the Nafion/Vulcan sample does not cause a similar cardinal suppression of the spectrum, which seems to be due to the lower conductivity of this composite.

The absence of ^{1}H lines in the region of 7.3 ppm for composites with TEG and Vulcan may indicate the disappearance of a large number of pores inside the Nafion matrix because of their filling with particles of modifying materials, or monomolecular enveloping of these particles with Nafion polymer fibers [26].

Fig. 3 shows the results of thermogravimetric analysis of composites. It can be seen that the thermal destruction of Nafion for the Nafion/TEG composite occurs in one stage – there is one stage of mass loss on the TG dependence, which corresponds to one pronounced peak on the differential termogravimetric curve (DTG). In the case of the Nafion/Vulcan composite, three areas of mass loss can be noted on the TG with three resolved peaks on the DTG (Peak temperatures are summarized in Table 2). This behavior may indicate the formation of a part of Nafion in the composite without the formation of spherical clusters containing sulfogroups on the inner surface, which is also confirmed by NMR data. Such structural features may be the reason for the increase in thermal stability.

The data in Fig. 3 and Table 2 demonstrate higher thermal stability of the Nafion/TEG composite compared to Nafion/Vulcan. The temperatures of the destruction peaks of these composites are still quite close, which is consistent with the proximity of the resonance frequencies in the NMR spectra.

4. Conclusion

Thus, the NMR studies of Nafion/carbon composites supplemented with thermogravimetry showed a strong influence of the carbon filler on the polymer. The presence of TEG and Vulcan leads to a change in the structural and physico-chemical characteristics of Nafion and increases its thermal stability due to the possible disappearance of a large number

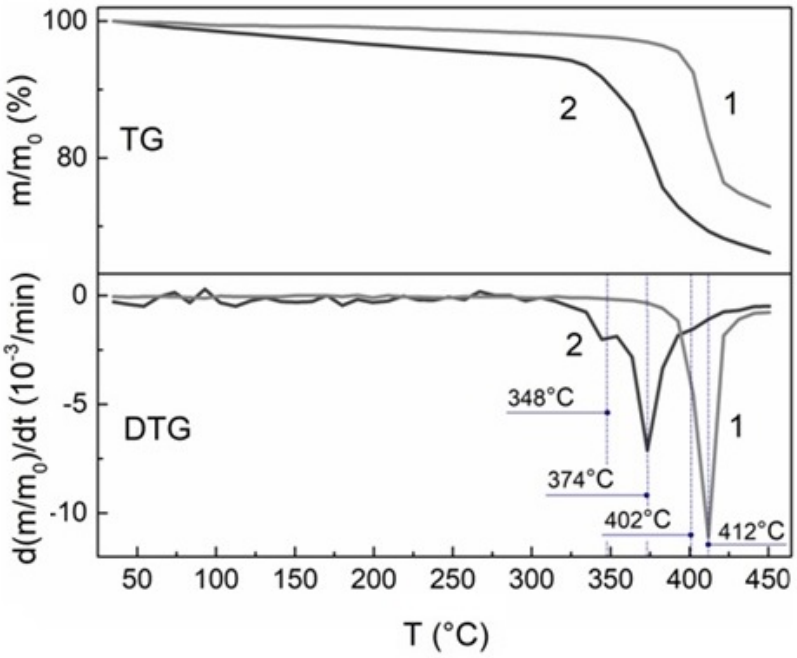

FIG. 3. Thermogravimetric and differential thermogravimetric destruction curves of Nafion when heated of composites Nafion/carbon material (wt. : wt.): 1 – Nafion/TEG 1:4; 2 – Nafion/Vulcan 1:4

TABLE 2. Nafion thermal destruction peak temperatures in Nafion/carbon composites (wt. : wt.): 1:4

Composite	Peak number	T, °C
Nafion/TEG	1	412
Nafion/Vulcan	1	348
	2	374
	3	402

of pores inside the Nafion matrix from - with particles of modifying materials or monomolecular coverage of these particles by polymer fibers Nafion. Besides, it was found that different carbon materials have different influence on the properties of Nafion.

References

[1] Tellez-Cruz M.M., Escorihuela J., Solorza-Feria O., Compañ V. Proton exchange m membrane fuel cells (PEMFCs): advancesand challenges. *Polymers*, 2021, **13**(18), P. 3064.

[2] Zatoń M., Rozière J., Jones D.J. Current understanding of chemical degradation mechanisms of perfluorosulfonic acid membranes and their mitigation strategies: a review. *Sustainable Energy Fuels*, 2017, **1**, P. 409–438.

[3] Bruijn F.A. de, Dam V.A.T., Janssen G.J.M. Durability and degradation issues of PEM fuel cell components. *Fuel Cells*, 2008, **8**(1), P. 3–22.

[4] Nechitailov A.A., Glebova N.V. Investigation of the stability of a nanocomposite of platinum carbon black and carbon nanotubes as an electrocatalyst of fuel cells. *Electrochemical energy*, 2013, **13**(4), P. 192–200 (in Russian).

[5] Nechitailov A.A., Glebova N.V. Mechanism of the effect of oxygen-modified carbon nanotubes on the kinetics of oxygen electroreduction on platinum. *Russian Journal of Electrochemistry*, 2014, **50**(8), P. 751–755.

[6] Grigoriev S.A., Bessarabov D.G. Fateev V.N. Degradation mechanisms of MEA characteristics during water electrolysis in solid polymer electrolyte cells. *Russian Journal of Electrochemistry*, 2017, **53**, P. 318–323.

[7] Siracusano S., Baglio V., Aricò A.S., Grigoriev S.A., Merlo L., Fateev V.N. The influence of iridium chemical oxidation state on the performance and durability of oxygen evolution catalysts in PEM electrolysis. *Journal of Power Sources*, 2017, **366**, P. 105–114.

[8] Pavlov V.I., Gerasimova E.V., Zolotukhina E.V., Don G.M., Dobrovolsky Yu.A., Yaroslavtsev A. B. Degradation of Pt/C electrocatalysts having different morphology in low-temperature PEM fuel cells. *Nanotechnologies in Russia*, 2016, **11**(11-12), P. 743–750.

[9] Moguchikh E.A., Alekseenko A.A., Guterman V.E. Novikovsky N.M., Tabachkova N.Yu., Menshchikov V.S. Effect of the composition and structure of Pt(Cu)/C electrocatalysts on their stability under different stress test conditions. *Russian Journal of Electrochemistry*, 2018, **54**, P. 979–989.

[10] Nechitailov A.A., Glebova N.V., Tomasov A.A., Krasnova A.O., Zelenina N.K. Study of the heterogeneity of a mixed-conducting electrochemical electrode. Technical Physics, 2019, **64**(6), P. 839–847.

[11] Ruiz-Perez F., López-Estrada S.M., Tolentino-Hernández R.V., Caballero-Briones F. Carbon-based radar absorbing materials: a critical review. *Journal of Science: Advanced Materials and Devices*, 2022, **7**(3), P. 100454.
[12] Ansari A., Akhtar M.J. High porous carbon black based flexible nanocomposite as efficient absorber for X-band applications. *Materials Research Express*, 2018, **5**(10), P. 105017.
[13] Wang Y., Gao X., Wu X., Luo C. Facile synthesis of Mn_3O_4 hollow polyhedron wrapped by multiwalled carbon nanotubes as a high-efficiency microwave absorber. Ceramics International, 2020, 46(2), P. 1560–1568.
[14] Min D., Zhou W., Qing Y., Luo F., Zhu D. Highly oriented flake carbonyl iron/carbon fiber composite as thin-thickness and wide-bandwidth microwave absorber. *J. Alloys Compd.*, 2018, **744**, P. 629–636.
[15] Cheng Y., Seow J.Z.Y., Zhao H., Xu Z.J., Ji G. A flexible and lightweight biomass-reinforced microwave absorber. *Nano-Micro Lett.*, 2020, **12**(1), P. 125.
[16] Du X., Wang B., Mu C., Wen F., Xiang J., Nie A., Liu Z. Facile synthesis of carbon-encapsulated Ni nanoparticles embedded into porous graphite sheets as high-performance microwave absorber. ACS Sustainable Chemistry and Engineering, 2018, **6**(12), P. 16179–16185.
[17] Zhao H., Han X., Li Z., Liu D., Wang Y., Wang Y., Zhou W., Du Y. Reduced graphene oxide decorated with carbon nanopolyhedrons as an efficient and lightweight microwave absorber. *J. Colloid Interface Sci.*, 2018, **528**, P. 174–183.
[18] Lu W.B., Wang J.W., Zhang J., Liu Z.G., Chen H., Song W.J., Jiang Z.H. Flexible and optically transparent microwave absorber with wide bandwidth based on grapheme. *Carbon*, 2019, **152**, P. 70–76.
[19] Mahanta U.J., Gogoi J.P., Borah D., Bhattacharyya N.S. Dielectric characterization and microwave absorption of expanded graphite integrated polyaniline multiphase nanocomposites in X-band. *IEEE Trans. Dielectr. Electr. Insul.*, 2019, **26**(1), P. 194–201.
[20] Zixuan Lei, Yuxi Song, Mingze Li, Shuaizhen Li, DianyuGeng, Wei Liu, Yu Cui, Haichang Jiang, Song Ma, Zhidong Zhang. Multi-carbon encapsulating soft-magnetic nanocomposite with environmentally adaptive wideband electromagnetic wave absorption, *J. Alloys Compd.*, 2023, **936**, P. 168216.
[21] Jiheng Ding, Panlin Liu, Min Zhou, Haibin Yu. Nafion-endowed graphene super-anticorrosion performance. *ACS Sustainable Chemistry and Engineering*, 2020, **8**(40), P. 15344–15353.
[22] Glebova N.V., Nechitailov A.A., Krasnova A.O. Thermal degradation of Nafion in the presence of nanostructured materials: thermally expanded graphite, carbon black, and platinum. *Russ. J. Appl. Chem.*, 2020, **93**(7), P. 1034–1041.
[23] Method of producing porous carbon material based on highly disintegrated graphite, Patent 2014116365/05 Russia: IPC C01B 31/04, Mazin V.I., N 2581382, Bull. N 11, 2016, 9 p.
[24] Kastsova A.G., Glebova N.V., Nechitailov A.A., Krasnova A.O., Pelageikina A.O., Eliseyev I.A. Electronic spectroscopy of graphene obtained by ultrasonic dispersion. *Tech. Phys. Lett.*, 2022, **48**(12), P. 60–62.
[25] Chen Q., Schmidt-Rohr K. 19F and 13C NMR signal assignment and analysis in a perfluorinated ionomer (Nafion) by two-dimensional solid-state NMR. *Macromolecules*, 2004, **37**(16), P. 5995.
[26] Lee W.-J., Bera S., Kim C.M., Koh E.-K., Hong W.-P., Oh S.-J., Cho E., Kwon S.-H. Synthesis of highly dispersed Pt nanoparticles into carbon supports by fluidized bed reactor atomic layer deposition to boost PEMFC performance. *NPG Asia Materials*, 2020, **12**(1), P. 40.

Submitted 22 March 2023; revised 28 March 2023; accepted 29 March 2023

Information about the authors:

Nadezhda V. Glebova – Ioffe Institute, 26 Politechnicheskaya str., St. Petersburg, 194021, Russia; ORCID 0000-0003-4519-0111; glebova@mail.ioffe.ru

Anton S. Mazur – St. Petersburg State University, 7-9 Universitetskaya emb., St. Petersburg, 199034, Russia; ORCID 0000-0002-2746-6762; a.mazur@spbu.ru

Anna O. Krasnova – Ioffe Institute, 26 Politechnicheskaya str., St. Petersburg, 194021, Russia; ORCID 0000-0001-6709-5559; krasnova@mail.ioffe.ru

Ivan V. Pleshakov – Ioffe Institute, 26 Politechnicheskaya str., St. Petersburg, 194021, Russia; ORCID 0000-0002-6707-6216; inanple@yandex.ru

Andrey A. Nechitailov – Ioffe Institute, 26 Politechnicheskaya str., St. Petersburg, 194021, Russia; ORCID 0000-0002-9895-6822; aan.shuv@mail.ioffe.ru

Conflict of interest: the authors declare no conflict of interest.